

# Conservative Linear Line Flow Constraints for AC Optimal Power Flow

Dmitry Shchetinin, Tomas Tinoco De Rubira, Gabriela Hug  
Power System Laboratory, ETH Zurich, Switzerland

**Abstract**—The AC optimal power flow problem is a non-convex optimization problem that is difficult to solve quickly and reliably for large-scale grids. To enable the application of efficient and robust solution algorithms, various linear approximations of the nonlinear system model are used. However, this may lead to solutions that are AC suboptimal or even infeasible. This paper proposes new linearization techniques for constructing accurate line flow constraints that reduce the complexity of the AC optimal power flow problem without compromising the solution quality. In particular, it investigates the shape of the nonlinear constraints in polar coordinates and presents methods for producing conservative linear approximations with a desired accuracy. Numerical experiments are performed on systems with 118, 300 and 1354 buses. Obtained results indicate that the proposed formulation leads to a significant decrease in the computation time while at the same time providing high quality approximations of the exact line flows.

**Index Terms**—linearization, optimal power flow, thermal limits

## I. INTRODUCTION

Optimization problems that arise in power system operation and planning are notorious for their complexity. Particularly, this includes the AC optimal power flow (OPF) problem, which was first introduced in [1] and has received a lot of attention over the years due to its practical importance [2]. This problem is non-convex and has a high dimension for realistic grids. Despite a large number of related studies, the development of an efficient and reliable solution algorithm to the AC OPF problem remains a challenge.

In order to simplify the original non-convex optimization problem, various approximations have been proposed. One widely used technique is the linearization of a steady-state system model, the so-called DC approximation [3]. The resulting DC OPF problem can be solved efficiently and the obtained solution is guaranteed to be globally optimal for the DC model. However, this solution may not be optimal or even feasible for the original AC model because of the inaccuracies introduced by the linearization [4]. Another way to approximate the AC OPF problem is to use recently proposed convex relaxations [5]. This is a promising research direction as these relaxations have been demonstrated to be tight for some test systems and grid topologies [6], [7]. However, in general there are no guarantees that convex relaxations will produce physically meaningful solutions for arbitrary power systems.

While recent years have witnessed significant improvements in nonlinear programming (NLP) techniques, available NLP solvers cannot always find a locally optimal point of the AC

OPF problem in reasonable time [8]. In fact, they are not guaranteed to find a feasible point even if one exists. The complexity of this problem lies in the constraint set. The nonlinear equality constraints represent the power flow equations and ensure that the solution satisfies Kirchoff's laws. The nonlinear inequality constraints represent operational limits such as restrictions on maximum line flows. Several studies have observed that including line flow limits in the problem formulation can significantly increase the computation time of NLP solvers [8]–[10].

Existing endeavors to approximate line flow constraints have been largely focused on the DC formulation. The least accurate yet most common approach is to only limit active power flows, which leads to linear inequality constraints. If additionally reactive power flows are modeled, the approximation better reflects reality [11]–[14]. However, the quality of such approximations is inherently limited because of the assumption that all bus voltage magnitudes are equal to one. In convex relaxations, line flow constraints can be modeled as quadratic constraints [15]. These approximations are accurate only when the relaxations to the power flow equations are tight, which is not generally true for all power systems.

The main contribution of this paper is twofold. First, it investigates the properties of nonlinear line flow constraints in polar coordinates for different operating conditions. Second, it presents computationally efficient methods for obtaining linear constraints that form a conservative approximation to each of the original nonlinear constraints. By substituting the nonlinear line flow constraints in the AC OPF problem with their linear approximations, one can reduce the problem complexity while ensuring that its solution is physically feasible. Using test systems of different sizes, the paper analyzes the accuracy of linear approximations and their effect on the computation time of state-of-the-art NLP solvers.

The rest of the paper is structured as follows. Section II presents a formulation of the AC OPF problem and Section III analyzes the properties of the nonlinear line flow constraints. Section IV describes proposed methods for obtaining conservative linear constraints. Section V presents the results of numerical experiments and Section VI concludes the paper.

## II. AC OPF FORMULATION

The AC OPF problem determines a physically and operationally feasible point that is optimal with respect to a given objective. This study focuses on determining an optimal generation dispatch that minimizes the total supply cost in the system. The supply cost  $C_i(P_{G_i})$  of  $i$ -th generator is modeled

This work was supported in part by the ETH Zurich Postdoctoral Fellowship FEL-11 15-1.

as a quadratic function of its active power output  $P_{G_i}$ :

$$C_i(P_{G_i}) := \alpha_i P_{G_i}^2 + \beta_i P_{G_i} + \gamma_i, \quad (1)$$

where  $\alpha_i, \beta_i, \gamma_i$  are machine-specific non-negative coefficients.

In general, decision variables for this problem can include both active  $P_G$  and reactive  $Q_G$  power outputs of generators. However, according to [16], simultaneous optimization of active and reactive power dispatch should be avoided as it can lead to line flows that are unreasonable from an engineering perspective. Therefore, this paper assumes that voltage magnitudes at generator buses are kept at given set-points and only  $P_G$  are the decision variables. The dependent variables include  $Q_G$  and complex bus voltages, which in polar form are described by their magnitudes  $V$  and phase angles  $\theta$ .

To ensure that the AC OPF solution satisfies Kirchhoff's laws, nodal power balance equations are included into the problem in the form of equality constraints. For bus  $i$ , active and reactive power mismatches  $W_{P_i}$  and  $W_{Q_i}$  are given by

$$W_{P_i} = P_{G_i} - P_{D_i} - \sum_{k \in \Omega_i} V_i V_k (g_{ik} \cos \theta_{ik} + b_{ik} \sin \theta_{ik}) \quad (2)$$

$$W_{Q_i} = Q_{G_i} - Q_{D_i} - \sum_{k \in \Omega_i} V_i V_k (g_{ik} \sin \theta_{ik} - b_{ik} \cos \theta_{ik}), \quad (3)$$

where set  $\Omega_i$  includes bus  $i$  and all buses connected to it,  $P_{D_i}$  and  $Q_{D_i}$  are active and reactive power demands at bus  $i$ ,  $g_{ik}$  and  $b_{ik}$  are the real and imaginary parts of the corresponding element of the admittance matrix, and  $\theta_{ik} = \theta_i - \theta_k$ .

The optimization problem also contains several types of inequality constraints. Bus voltage magnitudes and generator outputs have upper and lower bounds dictated by physical properties of the equipment and stability issues. Transmission lines and transformers have thermal limits, which are usually represented as upper bounds on the magnitude of apparent power flow  $S$  or line current  $I$ . This study uses the current limit because the current magnitude is directly related to the conductor's temperature. Transient stability limits are not considered in this study because they can be modeled simply as bounds on  $\theta_{ij}$  and do not increase the problem complexity.

The considered AC OPF problem is formulated as follows:

$$\underset{P_G, Q_G, V, \theta}{\text{minimize}} \quad \sum_{i \in \mathcal{N}_G} C_i(P_{G_i}) \quad (4a)$$

$$\text{subject to } W_{P_i} = 0, \quad i \in \mathcal{N} \quad (4b)$$

$$W_{Q_i} = 0, \quad i \in \mathcal{N} \quad (4c)$$

$$V_i = V_i^{\text{set}}, \quad i \in \mathcal{N}_G \quad (4d)$$

$$P_{G_i}^{\min} \leq P_{G_i} \leq P_{G_i}^{\max}, \quad i \in \mathcal{N}_G \quad (4e)$$

$$Q_{G_i}^{\min} \leq Q_{G_i} \leq Q_{G_i}^{\max}, \quad i \in \mathcal{N}_G \quad (4f)$$

$$V_i^{\min} \leq V_i \leq V_i^{\max}, \quad i \in \mathcal{N} \quad (4g)$$

$$I_i \leq I_i^{\max}, \quad i \in \mathcal{L}, \quad (4h)$$

where  $\mathcal{N}$ ,  $\mathcal{L}$ , and  $\mathcal{N}_G$  are the sets of all buses, lines, and generators, respectively,  $V_i^{\text{set}}$  is the voltage set-point of generator  $i$ . This problem is non-convex because of the nonlinear equality constraints (4b)-(4c) and non-convex inequality constraints on line flows (4h). To limit the scope of the paper, other control devices are not included in the formulation.

NLP solvers can generally handle linear inequality constraints more efficiently than nonlinear non-convex inequality constraints. Therefore, linearizing line flow constraints can enhance the performance of the solution algorithm, although the optimization problem remains non-convex because of nonlinear equality constraints. Note that if the linear approximations to constraints (4h) are conservative, the optimal solution to the AC OPF problem with linearized line flow constraints is guaranteed to be physically and operationally feasible.

### III. INVESTIGATION OF LINE FLOW CONSTRAINTS

In order to estimate the potential quality of linear approximations to nonlinear line flow constraints and develop linearization methods, this study first analyzes the shape of these constraints in polar coordinates.

#### A. General formulation

Consider a branch between buses  $i$  and  $j$  represented by a  $\pi$ -model with admittance  $g + jb$  and shunt susceptance  $b_s$  as shown in Figure 1. For the sake of simplicity, all formulations will be given for transmission lines but they can be easily extended to transformers. The current flowing through the line is a function of the complex voltages at both ends of the line. The current magnitude is given by:

$$I_{ij}(V_i, V_j, \theta_{ij}) = (\beta_1 V_i^2 + \beta_2 V_j^2 - 2V_i V_j (\beta_3 \cos \theta_{ij} - \beta_4 \sin \theta_{ij}))^{1/2}, \quad (5)$$

where  $\beta_1 := g^2 + (b + b_s)^2$ ,  $\beta_2 := g^2 + b^2$ ,  $\beta_3 := g^2 + b^2 + b_s b$ , and  $\beta_4 := b_s g$ . It is constrained to be below a given limit:

$$I_{ij}(V_i, V_j, \theta_{ij}) \leq I_{ij}^{\max}. \quad (6)$$

This inequality corresponds to constraint (4h) in the AC OPF problem formulation. It can be shown based on (5) that for all realistic line parameters for fixed  $V_i$  and  $V_j$  the value of  $I_{ij}$  reaches its minimum at  $\theta_{ij} \approx 0$  and increases monotonically with the increase of  $|\theta_{ij}|$ . The monotonicity property holds for  $|\theta_{ij}| \leq \frac{\pi}{2}$ , which is assumed to be a feasible region for steady-state operation if transient stability constraints are disregarded.

Let us refer to the set of all triples  $(V_i, V_j, \theta_{ij})$  for which inequality (6) holds as the feasible region of constraint (4h). The boundary of this region is given by all points that satisfy  $I_{ij}(V_i, V_j, \theta_{ij}) = I_{ij}^{\max}$ , i.e. when constraint (4h) becomes binding. At this boundary, the value of  $\theta_{ij}$  can be obtained from the values of  $V_i$  and  $V_j$  using:

$$\theta_{ij} = \arcsin \left( \frac{a_2 a_3 \pm a_2 \sqrt{a_2^2 + a_3^2 - a_1^2}}{a_2^2 + a_3^2} \right), \quad (7)$$

where  $a_1 = (I_{ij}^{\max})^2 - V_i^2 (g^2 + (b + b_s)^2) - V_j^2 (g^2 + b^2)$ ,  $a_2 = 2V_i V_j (g^2 + b^2 + b_s^2)$ , and  $a_3 = 2V_i V_j g b_s$ . The following conclusions can be made from analyzing equation (7):

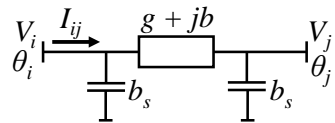


Fig. 1. Current magnitude for line between two generators

- If  $a_2^2 + a_3^2 - a_1^2 < 0$ , there exists no real-valued  $\theta_{ij}$  satisfying (7). This means that for a given pair of  $(V_i, V_j)$  the current magnitude  $I_{ij}(V_i, V_j, \theta_{ij})$  exceeds  $I_{ij}^{\max}$  for any  $\theta_{ij}$  and, therefore, this pair of  $(V_i, V_j)$  does not belong to the feasible region of constraint (4h).
- If  $a_2^2 + a_3^2 - a_1^2 > 0$ , there exist two values of  $\theta_{ij}$  that satisfy (7):  $\theta_{ij}^+$  and  $\theta_{ij}^-$ . Since for realistic transmission lines and transformers  $a_3$  is small,  $\theta_{ij}^- \approx -\theta_{ij}^+$ . Furthermore, the monotonicity of  $I_{ij}$  in  $|\theta_{ij}|$  means that for a given pair of  $(V_i, V_j)$  all values of  $\theta_{ij}$  in  $\theta_{ij}^- \leq \theta_{ij} \leq \theta_{ij}^+$  belong to the feasible region of constraint (4h).
- If  $a_2^2 + a_3^2 - a_1^2 = 0$ , there exists one value of  $\theta_{ij}$  that satisfies (7). Therefore, for a given pair of  $(V_i, V_j)$  only one value of  $\theta_{ij}$  satisfies constraint (4h).
- Finally, it follows from (6) that if the argument of  $\arcsin$  in (7) has magnitude greater than one, then for a given pair of  $(V_i, V_j)$  constraint (4h) is non-binding for any  $\theta_{ij}$ .

While in the analysis above no bounds on  $V_i$  and  $V_j$  were considered, in reality the bounds on bus voltage magnitudes always exist and are enforced by system operators. In the AC OPF formulation, these bounds are represented by constraints (4d) and (4g). To increase the quality of linear approximations to line flow constraints, one should consider the intersection of feasible regions of constraints (4d) and (4g)-(4h). If the resulting region is convex, it can be approximated arbitrarily well, otherwise its approximation quality depends on how non-convex the region is. The analysis of this region for different types of buses  $i$  and  $j$  is presented in the following subsections.

### B. Line between two generators

In the case of a line between two generator buses, both voltage magnitudes  $V_i$  and  $V_j$  are fixed and  $I_{ij}$  is a function of only one variable, namely,  $\theta_{ij}$ . Figure 2 shows the shape of this function for different line parameters and values of  $V_i$  and  $V_j$ . Depending on these parameters, constraint (4h) can be always violated, satisfied for any  $\theta_{ij}$  or satisfied for certain  $\theta_{ij}$ . Although the first two cases are unrealistic in practice, it is easy to check from (5) if they can occur for a given line. In the third case, the angles  $\theta_{ij}^-$  and  $\theta_{ij}^+$  at which constraint (4h) becomes binding are obtained from (7). As described above, constraint (4h) is satisfied for all  $\theta_{ij}$  between  $\theta_{ij}^-$  and  $\theta_{ij}^+$ .

### C. Line between load bus and generator

In the case of a line between a load bus and a generator bus,  $I_{ij}$  is a function of two variables, namely, phase angle difference  $\theta_{ij}$  and either  $V_i$  or  $V_j$ . The shape of this function is shown in Figure 3a for the case when  $V_j$  is fixed and  $V_i$  is allowed to vary  $\pm 15\%$  around its nominal value. Constraint

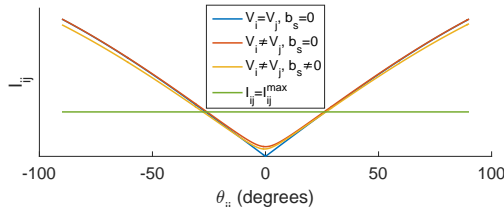


Fig. 2. Current magnitude for line between two generators

(4h) is binding for points  $(V_i, \theta_{ij})$  for which the surface  $\{ (V_i, \theta_{ij}, I_{ij}(V_i, \theta_{ij})) \mid (V_i, \theta_{ij}) \in \mathbb{R}_+ \times \mathbb{R} \}$  intersects the horizontal plane  $\{ (V_i, \theta_{ij}, I_{ij}^{\max}) \mid (V_i, \theta_{ij}) \in \mathbb{R}_+ \times \mathbb{R} \}$ . Figure 3a shows two such planes, which correspond to different values of  $I_{ij}^{\max}$ . The shaded areas in Figure 3b represent the feasible regions of constraint (4h) for each of these two values of  $I_{ij}^{\max}$ . The lower and upper bounds on  $V_i$  imposed by constraint (4h) can be computed by solving  $a_2^2 + a_3^2 - a_1^2 = 0$ , which results in a quadratic equation in  $V_i$  with roots  $V_i^l$  and  $V_i^u$ . As can be seen from Figure 3, when the value of  $I_{ij}^{\max}$  is small, these bounds may become tighter than the ones given by (4g).

The convexity of the feasible region can be determined from the shape of its boundary. Figure 4 shows the upper boundary curve for two values of  $I_{ij}^{\max}$ . The feasible region lies below the curve, which means that the region is convex when the curve is concave. Analyzing (7) reveals that the feasible region is convex for realistic thermal limits. Although the region can be slightly non-convex for very high thermal limits, its boundary is then attained at  $|\theta_{ij}| \geq \frac{\pi}{3}$ , which means that in practice this limit is not reached. The analysis for the case of fixed  $V_i$  is analogous and hence is omitted.

### D. Line between two load buses

The case of a line between two load buses is the most complex case because  $I_{ij}$  is a function of three variables, namely,  $V_i$ ,  $V_j$ ,  $\theta_{ij}$ , which is difficult to visualize. However, when constraint (4h) is binding,  $\theta_{ij}$  can be expressed as a function of  $V_i$  and  $V_j$  using (7). Figure 5 shows the resulting surface for two different values of  $I_{ij}^{\max}$  when both  $V_i$  and  $V_j$  are varied by  $\pm 15\%$  around their nominal values. As before, the feasible region is contained between the upper and lower part of the surface given by (7). As can be seen from Figure 5a, when the value of  $I_{ij}^{\max}$  is small, not all pairs of  $(V_i, V_j)$  in the box defined by  $0.85 \leq V_i \leq 1.15$  p.u.,  $0.85 \leq V_j \leq 1.15$  p.u. belong to the feasible region of constraint (4h). The reason is that once the difference between bus voltage magnitudes reaches a certain value, the current flowing through the line

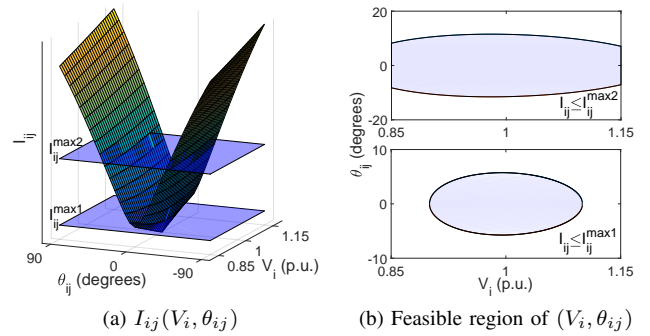


Fig. 3. Line flow constraint for line between a load and generator

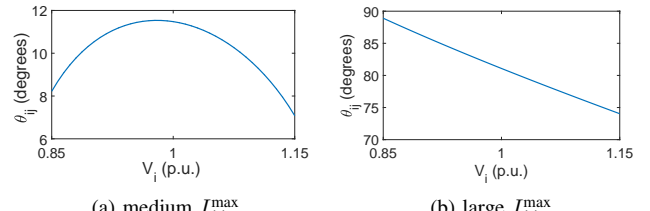


Fig. 4. Upper  $\theta_{ij}$  boundary for line between a load and generator

connecting these buses increases beyond  $I_{ij}^{\max}$  regardless of the value of  $\theta_{ij}$ . It can be shown from (7) that the projection of the feasible region of constraint (4h) onto the  $(V_i, V_j)$  plane is bounded by the following two linear inequalities:

$$V_j \leq \alpha V_i + \eta, \quad (8)$$

$$V_j \geq \alpha V_i - \eta, \quad (9)$$

where  $\alpha := \sqrt{\frac{g^2 + (b+b_s)^2}{g^2 + b^2}}$  and  $\eta = \frac{I_{ij}^{\max}}{\sqrt{g^2 + b^2}}$ . When either (8) or (9) becomes binding, it represents the boundary line at which the lower and upper parts of the surface given by (7) intersect (shown in Figure 5a in black). The value of  $\theta_{ij}$  is constant and close to zero for all points on this line. In addition, both the lower and upper parts of the surface contain a ridge, which is illustrated by a red curve in Figures 5-6. It follows from (7) that the projection of this ridge onto the  $(V_i, V_j)$  plane is given by the following straight line:

$$V_j = \alpha V_i, \quad (10)$$

which is parallel to both boundary lines. Moreover, the surface is symmetric with respect to the vertical plane passing through the ridge as well as the horizontal plane passing through boundary lines. These properties of the feasible region will be used for constructing its conservative linear approximation.

For a better illustration of the shape of the feasible region of constraint (4h), Figure 6 shows the upper part of the boundary of this region for two values of  $I_{ij}^{\max}$ . In this case, the region is not convex because the surface has directions of positive curvature for all values of  $I_{ij}^{\max}$ . For instance, analyzing (7) reveals that the projection of the ridge of the upper part of the surface onto either the  $(V_i, \theta_{ij})$  or  $(V_j, \theta_{ij})$  plane is convex for any value of  $I_{ij}^{\max}$ , which makes the feasible region non-convex. However, one can show that these non-convexities are negligible when bus voltage magnitudes have realistic bounds ranging from  $\pm 5\%$  to  $\pm 10\%$  of their nominal values.

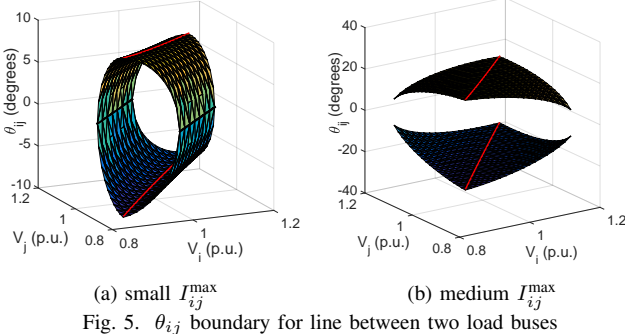


Fig. 5.  $\theta_{ij}$  boundary for line between two load buses

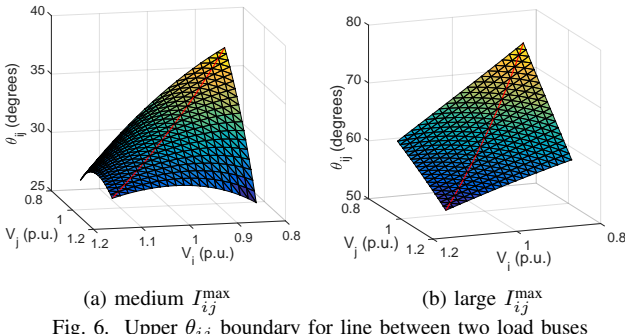


Fig. 6. Upper  $\theta_{ij}$  boundary for line between two load buses

#### IV. LINEARIZATION OF LINE FLOW CONSTRAINTS

As discussed in the previous section, for realistic operating points  $x \in \mathbb{R}^n$  the feasible region  $\mathcal{S}$  of line flow constraint  $h(x) \leq 0$  is close to convex. Therefore, it can be closely approximated by a polyhedron  $\mathcal{P} := \{x \mid Ax \leq b\}$ , where  $A \in \mathbb{R}^{m \times n}$  and  $b \in \mathbb{R}^m$ , provided that  $m$  is sufficiently high. This paper focuses on developing conservative approximations, which means that  $\mathcal{P} \subseteq \mathcal{S}$ . This guarantees that any solution to the AC OPF with linearized constraints is feasible for the original problem. Since in general there is more than one such approximation for a given  $m$ , another focus is on producing approximations that have a small error. To the best of the authors' knowledge, related works focus on constructing linear approximations of convex inequality constraints [10], whereas in this study the constraints are in general non-convex. Although linear approximations that are relaxations instead of conservative are not considered here, they can be obtained with the same methods described below. Due to space limitations, only a brief overview of the methods is presented.

It is important to mention that the computational complexity of all algorithms described in this section is  $\mathcal{O}(m)$ , where  $m$  is a desired number of linear constraints per nonlinear constraint. In addition, all constructed linear constraints are sparse.

##### A. Line between two generators

For all such lines, constraint (4h) can be substituted with:

$$\theta_{ij}^- \leq \theta_{ij} \leq \theta_{ij}^+, \quad (11)$$

where  $\theta_{ij}^-$  and  $\theta_{ij}^+$  are solutions to (7). Note that here there is no approximation error since (4h) and (11) have exactly the same feasible region with respect to  $\theta_{ij}$ .

##### B. Line between load bus and generator

In this case, linearization always produces a certain error because the boundary of the feasible region defined by (7) is nonlinear. To obtain a linear approximation to the upper part of the boundary curve (see Figure 4) for  $V_i^{\min} \leq V_i \leq V_i^{\max}$ , the following algorithm is used. First, the convexity of the feasible region is checked based on the sign of the boundary's curvature at any point in the interval. Since the feasible region lies below the boundary curve, it is convex when the curve is concave. If the region is convex, the lower and upper bounds  $V_i^l$  and  $V_i^u$  that constraint (4h) imposes on  $V_i$  are computed as described in Section III-C. The algorithm then constrains  $V_i$  to satisfy  $\tilde{V}_i^{\min} \leq V_i \leq \tilde{V}_i^{\max}$ , where  $\tilde{V}_i^{\min} = \max\{V_i^{\min}, V_i^l\}$  and  $\tilde{V}_i^{\max} = \min\{V_i^{\max}, V_i^u\}$ . An initial conservative approximation to the curve is given by the line connecting the points  $(\tilde{V}_i^{\min}, \theta_{ij}(\tilde{V}_i^{\min}))$  and  $(\tilde{V}_i^{\max}, \theta_{ij}(\tilde{V}_i^{\max}))$ . Next, a point on the curve with the maximum distance to the line is computed by a bisection algorithm. If this distance exceeds a given threshold, the approximation quality is deemed insufficient and the interval is split in two at the obtained point. This process is repeated until either the desired quality is achieved or the preset number of splits is reached.

If the region is non-convex, the boundary curve is approximated by only one line. To ensure that the approximation is conservative and has a high quality, the line is selected to be

tangent to the curve and parallel to the line connecting the points  $(V_i^{\min}, \theta_{ij}(V_i^{\min}))$  and  $(V_i^{\max}, \theta_{ij}(V_i^{\max}))$ .

It follows from (7) that the upper and lower parts of the boundary curve are symmetrical with respect to the line connecting the points  $(V_i^l, \theta_{ij}(V_i^l))$  and  $(V_i^u, \theta_{ij}(V_i^u))$ . Therefore, the approximation of the lower part of the boundary curve can be easily obtained by reflecting the approximation for the upper part of the curve over this line.

### C. Line between two load buses

In this case, the boundary surface of the feasible region is approximated by a set of planes. Due to non-convexity of the feasible region, the approximation error cannot be reduced arbitrarily close to zero regardless of the number of planes used. To construct a conservative approximation to the upper part of the boundary surface denoted by  $\theta_{ij}(V_i, V_j)$ , the algorithm described below is used, which takes as input the desired number of planes  $N$  in the approximation.

Initially, the set of values of  $V_i$  and  $V_j$  that satisfy both the voltage magnitude constraints (4g) and line flow constraint (4h) is determined. It represents a convex polytope  $\mathcal{Q}$  given by (4g) and (8)-(9). If  $\mathcal{Q}$  is empty, then problem (4a)-(4h) is infeasible. Otherwise, the linear approximation to  $\theta_{ij}(V_i, V_j)$  is constructed for all  $(V_i, V_j) \in \mathcal{Q}$  using a set of  $N$  planes.

The planes are obtained by computing the parameters of  $N-1$  lines along which the planes intersect. These intersection lines are chosen to be parallel to each other, hence they all have the same direction vector  $d := (d_1, d_2, d_3)$  in the space of tuples  $(V_i, V_j, \theta_{ij})$ . Therefore, to define each line one has to know  $d$  and a point through which the line passes. The projection of  $d$  onto the  $(V_i, V_j)$  plane is chosen to be parallel to the projection of the ridge given by (10), i.e. setting  $d_1 = 1$  yields  $d_2 = \alpha$ . The projections of the intersection lines onto this plane are spaced evenly, i.e. the projection of  $k$ -th line is

$$V_j = \alpha V_i + \gamma_{\min} + \frac{k}{N}(\gamma_{\max} - \gamma_{\min}), \quad (12)$$

where  $\gamma_{\min}$  and  $\gamma_{\max}$  are the minimum and maximum offsets of a line whose intersection with  $\mathcal{Q}$  is not empty. It can be shown that  $\theta_{ij}(V_i, V_j)$  restricted to any line (12) is a convex curve, which means that the tightest possible relaxed approximation to this curve is a line connecting its end points. This fact is used for computing the value of  $d_3$ :

$$d_3 = \sum_{k=1}^{N-1} \frac{\theta_{ij}(\bar{V}_i^{\max,k}, \bar{V}_j^{\max,k}) - \theta_{ij}(\bar{V}_i^{\min,k}, \bar{V}_j^{\min,k})}{\xi_k(\bar{V}_i^{\max,k} - \bar{V}_i^{\min,k})} \quad (13)$$

where  $(\bar{V}_i^{\min,k}, \bar{V}_j^{\min,k})$  is a point in  $\mathcal{Q}$  that has a minimum value of  $V_i$  and satisfies (12) for  $k$ -th line,  $(\bar{V}_i^{\max,k}, \bar{V}_j^{\max,k})$  is a point in  $\mathcal{Q}$  that has a maximum value of  $V_i$  and satisfies (12) for  $k$ -th line, and  $\xi_k$  is a weight coefficient proportional to  $\|(\bar{V}_i^{\max,k}, \bar{V}_j^{\max,k}) - (\bar{V}_i^{\min,k}, \bar{V}_j^{\min,k})\|_2$ . The idea behind this expression for  $d_3$  is to relate the approximation planes to the tangent planes of the surface and thus ensure that the approximation follows the shape of the nonlinear surface.

Once the direction vector has been obtained, one has to find a point through which each intersection line passes. Due to the shape of the upper part of the boundary surface, the approximation is guaranteed to be conservative if all intersection

lines lie below the surface for all  $(V_i, V_j) \in \mathcal{Q}$ . Therefore, to make the approximation as tight as possible while keeping it conservative, each line must touch the surface at exactly one point  $(V_i, V_j) \in \mathcal{Q}$ . This point for each line is determined by a bisection algorithm that samples the points satisfying (12) until it either finds one at which the tangent plane to the surface contains the direction vector  $d$  or converges to  $(\bar{V}_i^{\min,k}, \bar{V}_j^{\min,k})$  or  $(\bar{V}_i^{\max,k}, \bar{V}_j^{\max,k})$ . The parameters of all planes except the first and last one can be determined using the equations of adjacent intersection lines.

The first (last) plane must be a conservative approximation to the boundary surface for all points  $(V_i, V_j)$  that lie between the first (last) intersection line and the corresponding boundary of  $\mathcal{Q}$ . If this boundary is represented by a vertex  $(V_i^{\min}, V_j^{\max})$  (or  $(V_i^{\max}, V_j^{\min})$ ), the plane can be easily constructed using the vertex and the intersection line. However, if the boundary is represented by the boundary of either (8) or (9), a more elaborate procedure has to be used in order not to sacrifice the approximation quality. In this case, the first (last) plane is constructed such that it includes the corresponding boundary line and a point on the adjacent intersection line that has the largest value of  $\theta_{ij}$ . This may result in a situation where the actual intersection line between planes 1 and 2 (or  $N$  and  $N-1$ ) lies partly above the surface. In such case, a so-called “patch” plane is added to the approximation to guarantee its conservativeness. Due to the space limitations, a description of the algorithm that constructs this plane is not given.

## V. NUMERICAL EXPERIMENTS

### A. Experimental setup

Three test systems with 118, 300, and 1354 buses were considered in this study. Since they do not include thermal limits, the limits were artificially generated. Ten to twenty line limits for each system were made binding in order to check the impact of linearization on the optimal objective function value. The state-of-the-art NLP solvers KNITRO and SNOPT were considered. To enable a fair comparison, each solver had default settings and was provided with the gradient of the objective function and the Jacobian of the constraints.

### B. Experimental results

First, the quality of linear approximations was tested. A number of experiments was carried out using different values of voltage magnitude bounds, thermal limits, and line parameters. The obtained results confirmed that feasible regions of line flow constraints are close to convex. Figure 7 shows examples of the upper part of the boundary curve (in red) and its conservative approximations (in blue and green) for a line between a load and a generator. As can be seen from Figure 7b, even though the feasible region is non-convex for a high value of  $I_{ij}^{\max}$ , the non-convexity is negligible and the boundary is reached at values of  $\theta_{ij}$  that are not realistic for normal operation. The approximations of the upper part of the boundary surface for a line between two load buses are shown in Figure 8. As can be seen from Figure 8b, for a small value of  $I_{ij}^{\max}$  a “patch” plane (encircled by a dashed ellipse) might be needed. On average, for a line between two

TABLE I  
EXPERIMENTAL RESULTS FOR TEST SYSTEMS

System	Constr. type	Num constr.	$\Delta\text{Cost} (\%)$	Time (s)	
				SNOPT	KNITRO
118 bus	nonlin.	186	-	1.26	28.61
	lin. (x8)	984	0.0902	0.18	0.74
	lin. (x16)	2380	0.0043	0.27	0.95
300 bus	nonlin.	411	-	17.99	failed
	lin. (x8)	2826	0.0315	1.34	3.72
	lin. (x16)	5458	0.0053	1.88	4.46
1354 bus	nonlin.	1991	-	488.68	failed
	lin. (x8)	17840	0.0539	7.84	856.09
	lin. (x16)	35042	0.0076	17.28	903.50

load buses and bus voltage magnitudes varying  $\pm 10\%$  around the nominal values less than 16 constraints were needed to guarantee that whenever a linear constraint is active, the actual current magnitude is at least 98% of its given limit.

Next, for each test system linear approximations to thermal limit constraints were generated. Then, SNOPT and KNITRO were used to obtain a solution to three formulations of the AC OPF problem. The first formulation included nonlinear line flow constraints, while the other two instead included linear line flow constraints with on average 8 and 16 linear constraints per nonlinear constraint, respectively. The optimization time was measured for each combination of solver, formulation, and test system. The obtained results are presented in Table I. Despite a significant increase in the number of inequality constraints, SNOPT solved the AC OPF with linearized flow constraints on average ten times faster than the one with nonlinear constraints. KNITRO did not find a feasible point for the 300- and 1354-bus systems with nonlinear flow constraints but was able to solve all cases with linearized constraints. Table I also shows that more accurate approximations led to a smaller change in the optimal values of the total supply cost.

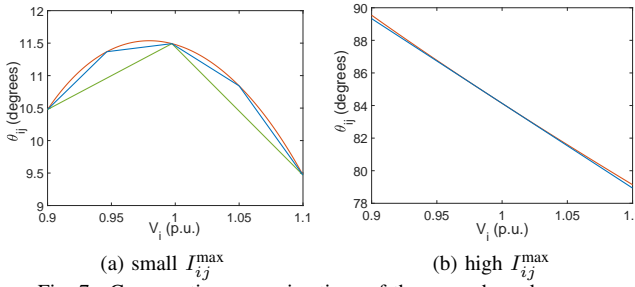


Fig. 7. Conservative approximations of the upper boundary curve

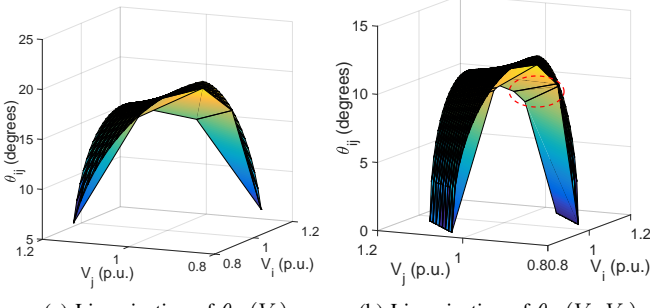


Fig. 8. Conservative approximations of the upper boundary surface

## VI. CONCLUSION

This paper proposes computationally efficient methods for producing conservative linear approximations to nonlinear line flow constraints in polar coordinates. It presents a detailed analysis of the shape of nonlinear line flow constraints, which demonstrates that these constraints are either convex or close to convex for realistic lines and operating limits and can be closely approximated with linear constraints. Incorporating the linear constraints into the AC optimal power flow problem instead of the original nonlinear constraints helps reduce the problem complexity without compromising the solution quality. Numerical experiments demonstrated that it is possible to achieve a high quality of such approximations by introducing a sufficient number of linear constraints. Although the resulting optimization problem has a larger size, the computation time of state-of-the-art NLP solvers SNOPT and KNITRO was significantly reduced. Future work includes considering other types of NLP solvers and constructing the relaxed approximations to the nonlinear line flow constraints.

## REFERENCES

- [1] J. Carpentier, “Contribution à l’étude du dispatching économique”, *Bulletin de la Société Française des Électriciens*, vol. 3, no. 8, pp. 431–447, 1962.
- [2] F. Capitanescu, J. L. Martinez Ramos, P. Panciatici, D. Kirschen, M. A. Marcolini, L. Platbrood, and L. Wehenkel, “State-of-the-art, challenges, and future trends in security constrained optimal power flow”, *Electric Power Systems Research*, vol. 81, no. 8, pp. 1731–1741, 2011.
- [3] B. Stott, J. Jardim, and O. Alsac, “DC Power Flow Revisited”, *IEEE Transactions on Power Systems*, vol. 24, no. 3, pp. 1290–1300, 2009.
- [4] T.J. Overbye, Xu Cheng, and Yan Sun, “A comparison of the AC and DC power flow models for LMP calculations”, in *Proceedings of the 37th Annual Hawaii International Conference on System Sciences*, 2004.
- [5] Subhonnmesh Bose, Steven H. Low, Thanchanok Teeraratkul, and Babak Hassibi, “Equivalent Relaxations of Optimal Power Flow”, *IEEE Transactions on Automatic Control*, vol. 60, no. 3, pp. 729–742, 2015.
- [6] Javad Lavaei and Steven H. Low, “Zero Duality Gap in Optimal Power Flow Problem”, *IEEE Transactions on Power Systems*, vol. 27, no. 1, pp. 92–107, Feb. 2012.
- [7] Masoud Farivar and Steven H. Low, “Branch Flow Model: Relaxations and Convexification—Part I”, *IEEE Transactions on Power Systems*, vol. 28, no. 3, pp. 2554–2564, Aug. 2013.
- [8] Florin Capitanescu and Louis Wehenkel, “Experiments with the interior-point method for solving large scale Optimal Power Flow problems”, *Electric Power Systems Research*, vol. 95, pp. 276–283, Feb. 2013.
- [9] P. Lipka, R. O’Neill, and S. Oren, “Developing line current magnitude constraints for IEEE test problems”, Tech. Rep., FERC, 2013.
- [10] M. Pirnia, R. O’Neill, P. Lipka, and C. Campaigne, “A computational study of linear approximations to the convex constraints in the iterative linear IV-ACOPF formulation”, Tech. Rep., FERC, 2013.
- [11] S. Grijalva, P. W. Sauer, and J. D. Weber, “Enhancement of linear ATC calculations by the incorporation of reactive power flows”, *IEEE Transactions on Power Systems*, vol. 18, no. 2, pp. 619–624, May 2003.
- [12] Joshua A. Taylor and Franz S. Hover, “Linear Relaxations for Transmission System Planning”, *IEEE Transactions on Power Systems*, vol. 26, no. 4, pp. 2533–2538, Nov. 2011.
- [13] Carleton Coffrin and Pascal Van Hentenryck, “A Linear-Programming Approximation of AC Power Flows”, *INFORMS Journal on Computing*, vol. 26, no. 4, pp. 718–734, May 2014.
- [14] C. Coffrin, P. Van Hentenryck, and R. Bent, “Approximating line losses and apparent power in AC power flow linearizations”, in *2012 IEEE Power and Energy Society General Meeting*, July 2012, pp. 1–8.
- [15] Carleton Coffrin, Hassan L. Hijazi, and Pascal Van Hentenryck, “The QC Relaxation: A Theoretical and Computational Study on Optimal Power Flow”, *IEEE Transactions on Power Systems*, vol. 31, no. 4, pp. 3008–3018, July 2016.
- [16] B. Stott and O. Alsac, “Optimal power flow: Basic requirements for real-life problems and their solutions”, 2012.